Cathodic control using cellular automata approach

Mariem Zenkri, Dung Di Caprio, Fayçal Raouafi, Damien Féron

Cathodic control using cellular automata approach

M. Zenkri[a,b,c], D. di Caprio[b,*], F. Raouafi[a,c], D. Féron[d]

[a] *LPC2M, IPEST, Route Sidi Bou Said, B.P:51 2075 La Marsa, Tunisie*
[b] *Chimie ParisTech, PSL Research University, CNRS, Institut de Recherche de Chimie Paris (IRCP), Paris*
[c] *Faculté des Sciences de Bizerte, 7021 Jarzouna, Université de Carthage, Tunisie*
[d] *Den-Service de la Corrosion et du Comportement des Matériaux dans leur Environnement (SCCME), CEA, Université Paris-Saclay, Gif-sur-Yvette, France*

Abstract

We present a stochastic three dimensional cellular automata model of aqueous corrosion. We consider the cathodic reaction with dissolved oxygen and different concentrations of the oxidizer. We study the role and the stability of the passive layer and its effect on the kinetics, surface morphology and roughness of the metallic surface. The model considers balanced spatially separated anodic and cathodic reactions and is capable of illustrating the cathodic control of the corrosion rate. Besides the electrochemical reactions, we take into account ionic diffusion, acido/basic neutralization. Results are compared to aqueous corrosion of Fe in near neutral solution.

Keywords: corrosion, cathodic control, dissolved oxygen, cellular automata, passivation

1. Introduction

The evaluation of the damage of a material, due to the action of corrosion, represents an important challenge on both economic and scientific levels, [1, 2]. Limiting the degradation of metals will enhance their durability leading to financial gain and avoiding costs which can reach 4% of international GDP [1, 3]. Corrosion Engineering is mainly focused on practical advances and relies on collecting existing data about corrosion in view of improving corrosion protection [4]. In contrast, experimental or theoretical scientific studies aim at modelling for understanding and predicting corrosion rates in order to adjust and optimize materials composition and resistance.

In this article, we focus on aqueous corrosion. Aqueous corrosion occurs as a result of a combination of chemical and electrochemical reactions on a metal surface including electronic transfer between two regions associated to the anodic and cathodic reaction, plus an ionic diffusion between the different species in the solution surrounding the metal.

*Corresponding author

Anodic reactions are generally related to metal oxidation. Cathodic reactions depend on the type of the oxidant present in the solution. For aqueous corrosion and anaerobic systems, only a reduction of H^+ or the reduction of the water molecules takes place. In the case of aerobic systems, called also aerated systems, the reduction reaction is set by the amount of dissolved oxygen (DO) present in the electrolyte. As shown in many works, DO in solution has an important effect on the corrosion rate. For an example, in the case of carbon steel, it has been reported that the corrosion rates of the material are higher in solutions with the presence of DO independently of the type of the solution like hydrolic acid, sulphyric acid or sodium chloride (3.5% NaCl) [5] .

During corrosion, the metal can be covered by an oxide layer formed by the metal itself as a consequence of the anodic reaction [6]. The formation of the passive layer or its dissolution taking place at random locations over the surface leads to an heterogeneous morphology of the surface and the appearance of surface roughness. This roughness is considered often to have as a major influence on the kinetics of the deterioration of a metal. Many studies have been completed to evaluate the relationship between the surface roughness and the kinetics of the corrosion process using several methods. For magnesium alloy AZ91 [7], stainless steels [8, 9], copper [10], aluminum or titanium-based alloys [11] an increase in the surface roughness, increases the susceptibility to localized corrosion. Typically, the general and localized corrosion behaviour of alloys would depend on their passivation properties. Hence, it is important to know the passivation behaviour of alloys with different surface finish to correlate the surface roughness to their general corrosion and pitting tendency [12, 7]. For metals with the ability to form a passive layer, a decrease in surface roughness increases the corrosion resistance but for the ones with no passive film, the opposite trend has been observed e.g. mild steel [13] and AE44 magnesium alloy [12]. In fact, the surface roughness increases the specific area of the metal surface in contact with the electrolyte.

In this work, we have considered cellular automata modelling. The cellular automata modelling is a powerful and successful method in modelling the evolution of a system modelled by a discrete lattice decomposed into cells which evolve according to a set of rules and depending on the cells' neighborhood. This type of modelling is based on a discretization in both space, time and consideration of physical states and chemical species as different states of the cell. Cellular automata modelling of corrosion started with P. Meakin et al. in 1993, [14] and after that, different algorithms have been developed using cellular automata in the framework of corrosion processes studies. An overview of cellular automata modelling of the corrosion processes can be

found in [15, 16]. In the present work, we use a three dimensional corrosion model with spatially separate anodic and cathodic reactions and accounting of acido-basic species in solution [17, 18, 19]. A new feature is introduced with accounting for cathodic reaction taking place with dissolved oxygen DO.

The paper is organised as follows. We first present the model and its cellular automata implementation, in particular concerning the representation of small oxygen concentrations. Then we present the differents results concerning the corrosion rate and the roughness as a function of different effects like passivation or oxygen concentration. Then a small section compares model results to experimental values for the corrosion rate. Finally, summary and conclusions are given.

2. Model

2.1. Cellular automata model

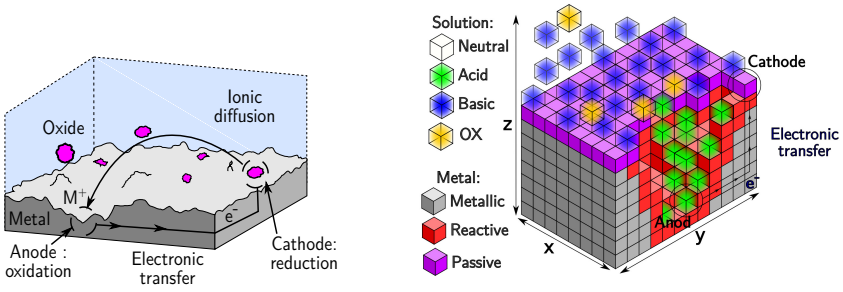

Figure 1: Cellular automata model (right) based on the corrosion scenario (left)

Cellular automata (CA) modelling is based on a simplified reality where the system is modelled on a lattice by regular cells which can take a finite number of states representing in our case chemical species in possibly different physical states, see figure 1. In the present model we take for simplicity a cubic lattice. The states in this model are the following. For solid sites, we have metal sites which are subdivided into reactive sites of the metallic surface R and bulk metal M and also oxide or passive sites P. Metallic R sites can host anodic and cathodic reactions, whereas oxide sites can only host cathodic reations. The solid material is immersed in an electrolyte. For the solution states, we distinguish acid A (i.e. H^+), basic B (i.e. OH^-), neutral N solution sites and for this aerated system we also take into account dissolved oxygen sites DO.

In the CA, the evolution of the cells is given by rules in relation with the neighbourhood of the evolving cell. In this work, Moore neighbourhood is taken with 26 neighbours in the

three dimensional space. This extended neighbourhood allows for detailed accounting of a cell's neighbourhood. Here, the evolution rules for the cells account for two processes: diffusion and chemical/electrochemical reactions. In particular, we will consider the possibility of having anodic and cathodic electrochemical half-reactions in spatially separated sites. We make sure when executing a pair of half-reactions, that they are paired i.e. the anodic and cathodic sites are connected by metal to ensure the electronic connectivity between those sites. This is achieved by using the burning algorithm detailed in [20].

For comparison with the literature, we will now consider experimental systems and results taken from [21, 22].

2.2. Diffusion

We first express diffusion in terms of the CA. The diffusion of species in solution follows a random walk which verifies [23]:

$$\langle r^2 \rangle = 2\,d\,D\Delta t_{\text{diff}} \tag{1}$$

$\langle r^2 \rangle$ is the average of the square of the distance traveled in a time Δt_{diff}, $d = 3$ is the space dimension and D is the diffusion coefficient. In the CA, a site in solution site diffuses by swapping content with an other solution type cell in it's neighbourhood, this rules has an exception detailed below in the case an acidic and basic cell are adjacent, in this case a reaction takes place. In the Moore neighborhood, the average distance of an elementary displacement in all possible directions gives [17]

$$\langle r^2 \rangle = 2.0769\,a^2 \tag{2}$$

where a is the characteristic length of a cell, we will hereafter take $a = 10\,\mu m$.

For comparison with results in [22], we consider systems at 50° C. In these conditions, diffusion coefficient for DO is $4.50\,10^{-5} cm^2 s^{-1}$ [24]. For H^+, OH^- we have diffusion coefficients of the order $7.3\,10^{-5} cm^2 s^{-1}$ [17, 25]. To simplify the simulation and keep the same diffusion algorithm for all the species in solution, we will take the identical value for corresponding to the diffusion of DO. In this paper, we will focus on the effect of DO. With the above diffusion coefficient and a characteristic size of a cell of $10\,\mu m$, and according to equation (1), we have the value of a single diffusion time step $\Delta t_{\text{diff}} = 1.54\,10^{-2} s$. Relation with the corrosion time step, is set by the parameter N_{diff} as $\Delta t_{\text{corr}} = N_{\text{diff}} \Delta t_{\text{diff}}$. We considered simulations with typically $2.\,10^5$ corrosion time steps, and study the cases with $N_{\text{diff}} = 100$, 250, 500 and 1000. This corresponds,

respectively to 85.3, 212, 427, 853 hours of a macroscopic real simulated time. In the following, we choose to represent time in number of corrosion time steps units. From a computational point of view, the size of the cellular automata being of the order $\approx 10^8$ sites, simulations can take from several days to several weeks with parallel algorithms in CUDA environment on NVIDIA TESLA K80 cards.

2.3. Chemical, electrochemical reactions

As mentionned above, a reaction occurs when diffusing acidic A (H^+) and basic B (OH^-) sites meet in solution and react by annihilating and are replaced by a neutral sites. Note that in the initial state, at time $t = 0$, the metal is immersed into a neutral solution, when corrosion takes, acidic and basic sites can be produced as detail in the following.

Besides diffusion, sites can react and change chemical or electrochemical state depending on the neighbourhood. In table 1, we present the possible electrochemical reactions which we consider to contribute to the corrosion process. They occur on the metallic surface. The electrochemical reactions for the metal involve a single electron, however the model can easily be generalized to any number of electrons.

Table 1: Electrochemical reactions

Chemical reactions	Cellular automata rules	Environnement	Probabilities
Anodic			
$M + H_2O \longrightarrow MOH_{aq} + H^+ + e^-$	Metal $\longrightarrow$ Acid	Acid, Neutral	P_{sse}
$M + OH^- \longrightarrow MOH_{solid} + e^-$	Metal + Basic $\longrightarrow$ Passif + Neutral	Basic	P_{sse}
Cathodic			
$O_2 + 4H^+ + 4e^- \longrightarrow 2H_2O$	Surf + DO + Acid$\longrightarrow$ Surf + Neutral	Acid, Neutral	P_{sse}
$O_2 + 2H_2O + 4e^- \longrightarrow 4OH^-$	Surf + DO +Neutral $\longrightarrow$ Surf + Basic	Basic	P_{sse}
Spatially Joint (SJ) reactions			
$M + \frac{1}{2} H_2O + \frac{1}{4} O_2 \longrightarrow MOH_{aq}$	Metal + DO $\longrightarrow$ Neutral	Acid ou Neutral	P'_{oxi}, P_{oxi}
$M + \frac{1}{2} H_2O + \frac{1}{4} O_2 \longrightarrow MOH_{solid}$	Metal + DO $\longrightarrow$ Passive	Basic	1
$MOH_{solid} \longrightarrow MOH_{aq}$	Passif$\longrightarrow$ Neutral	Acid ou Neutral	P'_{oxi}, P_{oxi}

Surf = Metal or Oxide (passive metal)

The program accounts for cathodic reaction with oxygen in different environments depending on the presence and number of a H^+ sites in the neighbourhood.

- Anodic reactions:

For Acidic and neutral environment, we have metal oxidation and cation hydrolysis. In basic environment, an insoluble hydroxide is formed and precipitates on the surface. In both environments, we have either a production of H^+ or a consumption of OH^- which corresponds to a decrease of the value of the pH thus acidification of the solution.

• Cathodic reactions:

We have reduction of DO presented differently according to the environment: acidic, neutral or basic. We have respectively either a consumption of H^+ ions or a production of OH^- ions. In both cases there is an increase in pH i.e. basification of the solution locally.

2.4. Representing DO concentration in the CA

In oxygenated water, hematite (Fe_2O_3) or ferric hydroxydes ($Fe(OH)_3$ or FeOOH) are the main corrosion products. But in water without dissolved oxygen or low oxygen concentration, magnetite (Fe_3O_4) or ferrous hydroxydes ($Fe(OH)_2$) are the corrosion products. To simplify the modelling, we choose to form the same oxide, magnetite Fe_3O_4 whatever is the oxygen concentration and compare with experimental results in [22] and consider the following chemical reaction:

$$\mathrm{Fe} + \frac{2}{3}\,\mathrm{O_2} \longrightarrow \frac{1}{3}\,\mathrm{Fe_3O_4}. \tag{3}$$

In this article 50°C systems are considered. The observed oxygen concentrations are approximately from 1 to 8 ppm ($ppm = mg/kg$). In the following, we will take a typical value of 6 ppm of DO in solution. We present hereafter how to represent this small concentration within the cellular automata.

For quantitative evaluation in the CA, two steps have to be considered. First we need to evaluate the quantity of DO in a site considering that in the CA there is stoechiometric reaction of a single DO site with a single metal site according to the cellular automata rules in table 1. Second given the quantity of DO in a single site, we have to estimate the number of DO sites to represent on average the 6 ppm concentration of DO in solution.

To evaluate the first step, we use the molar volume of iron at room temperature is $v_m^{\mathrm{Fe}} = 7.09\,10^{-6} m^3 mol^{-1}$. The numbers of moles of iron in a cell is then $n_{\mathrm{Fe}} = \dfrac{a^3}{v_m^{\mathrm{Fe}}}$ which reacts with $n_{\mathrm{O_2}} = \dfrac{2}{3} n_{\mathrm{Fe}}$ of DO according to equation (3). This gives us the DO content of a cell.

We now consider the second step, to estimate the concentration of DO sites to represent the $6\,ppm = 6\,mg/kg$ concentration. Considering the molar mass of dissolved oxygen is $32 gmol^{-1}$, a site in these conditions will hold $n_{DO} = 6 \times \dfrac{(10^{-4})^3}{32.\,10^3}$ moles. The dilution rate of 6 ppm corresponds to a dilution in number of sites of

$$\frac{n_{DO}}{n_{\mathrm{O_2}}} = 1.987\,10^{-6} \approx 2\,10^{-6} \tag{4}$$

In the simulation, the DO concentration is fixed by imposing a fixed concentration on the last top plane of the simulation boxwitch is parallel to the metallic surface, figure 2. Systems simulated

have lattice size (1024, 1024, 128) sites along x, y, z directions. The last top plane has dimensions 1024×1024 sites, therefore the dilution rate corresponds to approximately keeping two sites in the last top plane as shown in figure 2 at each simulation step. This plane is furthest from the reacting surface and allows to simulate the diffusive layer effect. By diffusion i.e. random walk, the oxygen sites are then free to leave this plane and diffuse in the rest of the volume to reach the reactive surface and a cathodic reaction can take place. Being consumed at the metallic surface there concentration is not fixed in the volume, there is profile.

Note that the above representation of a low DO concentration from few highly concentrated DO cells may appear unusual. We recall this is the consequence of the CA representation with a one to one cell reaction between metal and DO. It must be emphasized that only the average collective effect of the DO sites over a large number of time steps has a meaning. The small number of events due to the low DO concentration is compensated by a large simulation time for which the accumulation of corrosion events spread over the entire surface leads to an average effect which is representative.

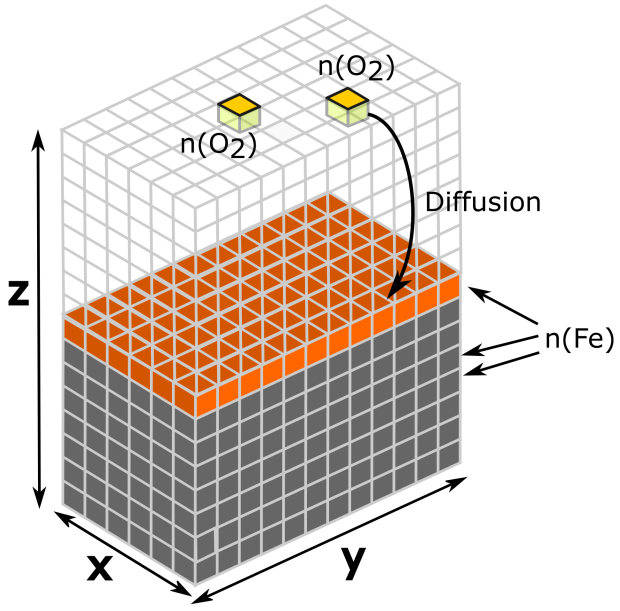

Figure 2: Cellular automata with fixing a density of two sites of oxygen in the last plane $n(O_2)$ and $n(Fe)$ refers to, respectively, the number of moles of oxygen and iron in one site.

Finally, also note that due to the low *ppm* concentration of DO, anodic corrosion half-reactions

occur very seldom, we are in a cathodic controlled corrosion. In this case, no accumulation of acidic and basic sites is expected. Indeed, after having been produced by the anodic or cathodic reactions, acidic and basic sites have sufficient time to diffuse away from the metallic surface where they are produced. This is contrast with conditions investigated in previous papers, where the absence of cathodic control allowed for much faster corrosion rates [17, 18, 19]. Thus with a small amount of DO the transition to the localized corrosion regime presented in these papers is more difficult to occur. We therefore focus on studying the corrosion and passivation phenomena only in neutral medium with a probability P_{oxi} which controls the dissolution of oxides in this environment.

2.5. Studied quantities

In what follows, we will calculate different quantities:

• The corrosion rate v_{corr}: equal to the derivative of the corrosion height loss Δh_{loss} in a units divided by the corrosion elementary time Δt_{corr}, quantity of interests for engineers. As for each corrosion step, we execute a number N_{diff} of diffusion steps, the corrosion rate is calculated using :

$$v_{corr} = \frac{a\Delta h_{loss}}{\Delta t_{\text{corr}}} = \frac{a\Delta h_{loss}}{N_{\text{diff}}\Delta t_{\text{diff}}} \tag{5}$$

where a is the lattice site characteristic size.

• The chemical roughness σ_{chem}: equal to the number of surface reactive R and P sites, which represent also the number of cathodic sites N_c, divided by the surface sites in a plane [17, 26, 27]

$$\sigma_{chem} = \frac{N_c}{N_x \times N_y} \tag{6}$$

For a rough surface, this quantity becomes larger than one and being related to the number of reactive sites, as it is the interface between the metal and the solution, it is directly related to the kinetics of corrosion.

For both quantities, we will study the effect of the parameter N_{diff} given in the equation (5). We will also study the effect of the dissolution probability in neutral environment: P_{oxi} on the corrosion regime.

3. Results

3.1. Oxide stability and corrosion rate

In this section we investigate the relationship between the oxide stability and the corrosion kinetics by varying the dissolution probability: P_{oxi}.

In figure 3, we present the evolution of the corrosion rate for different values of the dissolution probability and for given values of diffusion step N_{diff}. We observe that the corrosion rate increases at the beginning of the process, until it reaches a stable state (stationary regime) for all given values of N_{diff}: 100, 250, 500 and 1000. This can be understood if account for the increase of chemical roughness which is presented below and reflects the increase in the available number of reacting sites. Also, the higher the value of P_{oxi} the more we dissolve oxide sites on the surface limiting the passivation effect of the oxide leading to a faster corrosion rate. For $P_{\text{oxi}} = 0.01$ and 0.1, the difference is insignificant the dissolution of the oxide being for both values quantitative, there is no passivation. The system reaches a limiting corrosion rate fixed only by the cathodic reaction controled by the diffusion of DO.

3.2. Stationary corrosion rate and diffusion

In the previous paragraph, we have seen that the kinetic of the corrosion process varies with the dissolution rate of the oxide P_{oxi} in a similar way for all values of the diffusion rate N_{diff}. In the differents plots, it appears that the value of the corrosion rate decreases with increasing the value of N_{diff} as expected as the diffusion time is constant and N_{diff} sets the corrosion time which increases linearly with this parameter. In other words the corrosion rate is inversely proportional to N_{diff}. This is verified in figure 4 where we plot for different values of P_{oxi}, the corrosion rate of the stationary regime as a function of $\frac{1}{N_{\text{diff}}}$ where we observe a linear behavior for all values of P_{oxi}. But we also note that the linear behaviour corresponds to different slopes, showing the effect of P_{oxi} on the corrosion kinetics. This is also expected as low values of P_{oxi} imply passivation therefore lower corrosion kinetics. Again, the cases $P_{\text{oxi}} = 0.01$ and 0.1 corresponding to high oxide dissolution exhibit no passivation and cathodic control from *DO* diffusion.

3.3. Chemical roughness

During the corrosion process, the reactive surface in contact with the solution evolves with the surface roughness. This roughness is due to both: corroded sites and sites protected by passivation preventing corrosion. Both type of sites being stochastically distributed on the surface contribute to an inhomogeneous corrosion of the surface. In figure 5, we note that

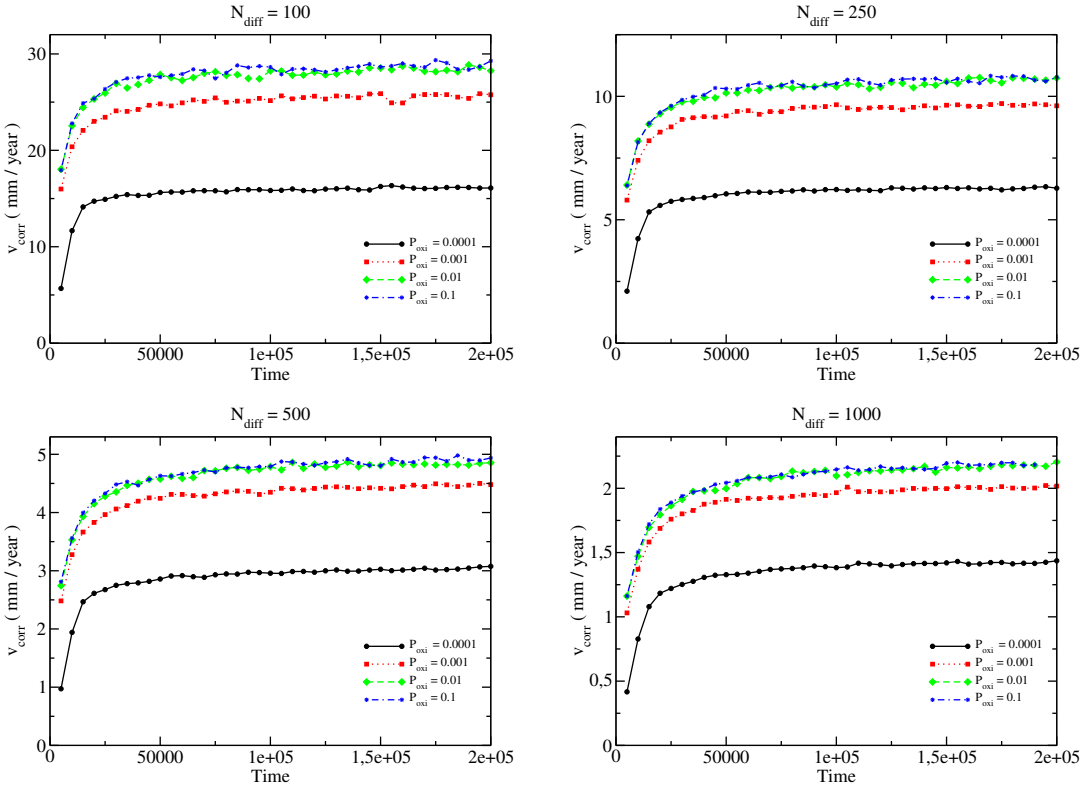

Figure 3: Corrosion rate for $N_{\mathrm{diff}} = 100, 250, 500$ and 1000 and different values of P_{oxi}.

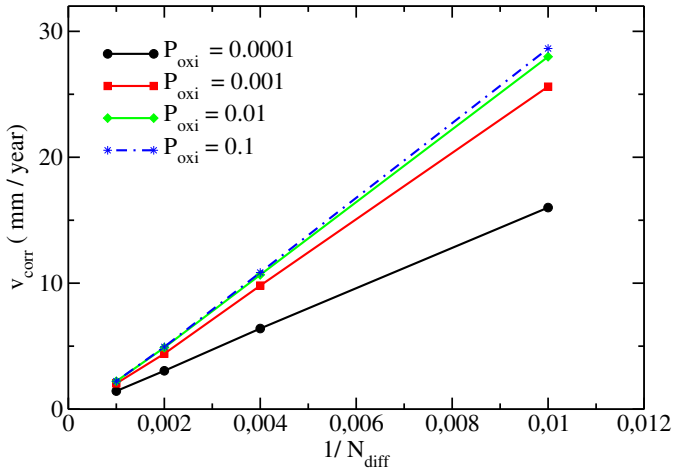

Figure 4: Corrosion rate as a function of $1/N_{\mathrm{diff}}$ and different values of P_{oxi}.

this roughness σ_{chem} follows the same evolution than the corrosion rate as a function of time although the magnitude of the change is different. There is a transition to a steady state for times comparable to those of the corrosion rate. Note that the stationary value of the roughness

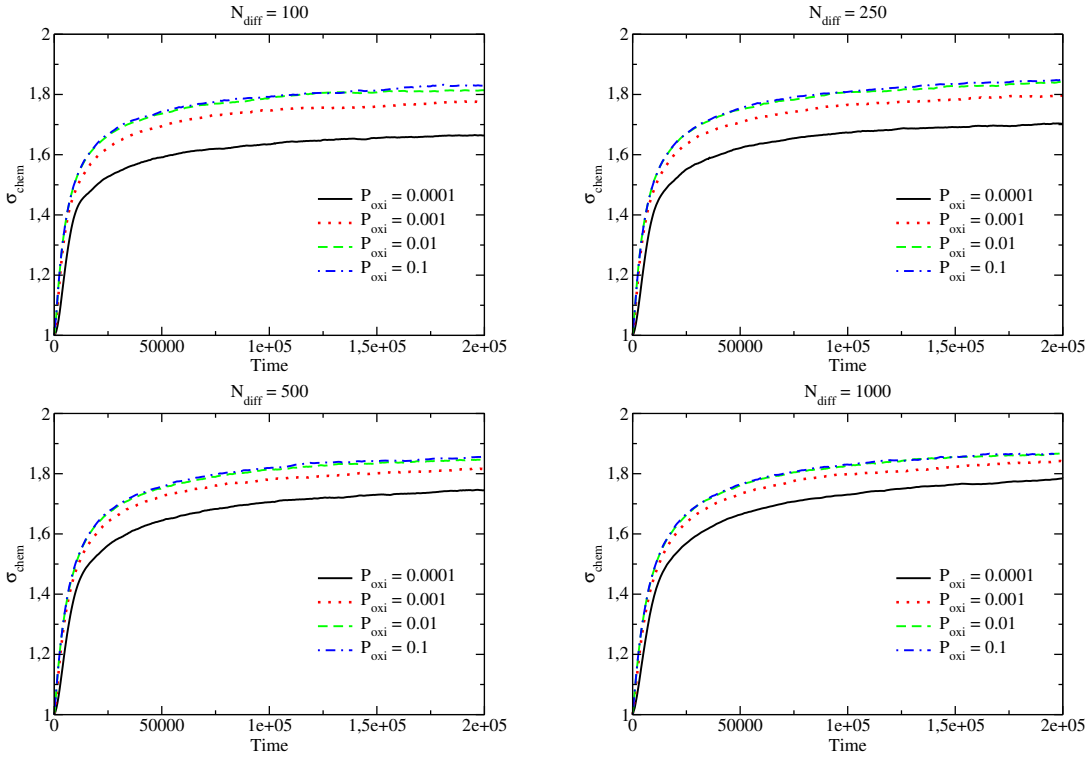

Figure 5: Chemical surface roughness σ_{chem} with $N_{\text{diff}} = 100, 250, 500$ and 1000 and different values de P_{oxi}.

is weakly influenced by the diffusion time step N_{diff}, so it has a small dependence to the corrosion rate. Whereas increasing the probability of dissolution of the oxide P_{oxi}, the chemical roughness is slightly increased. Nonetheless, both effects remain relatively weak and in all cases there is an increase in number of reacting sites which can be correlated to an increase in corrosion. In the absence of passivation $P_{\text{oxi}} = 0.01$ and 0.1, the roughness reaches a limit as shown before for the corrosion rate.

3.4. Passivation

During the simulation, at each time step the number of anodic and cathodic sites are recorded. From Table 1, we recall that anodic reactions can occur only on the metal sites whereas cathodic reactions can take place on both the metal and the oxide sites. The difference between cathodic

and anodic sites is then equal to $n_{\rm ox}$ the number of oxide sites on the surface and provides information on the passivation state of the surface.

The evolution of $n_{\rm ox}$ is presented first in plots at fixed $N_{\rm diff}$ and different values of $P_{\rm oxi}$, then at fixed $P_{\rm oxi}$ for different values of $N_{\rm diff}$. Figure 6 shows the evolution of the number of oxide

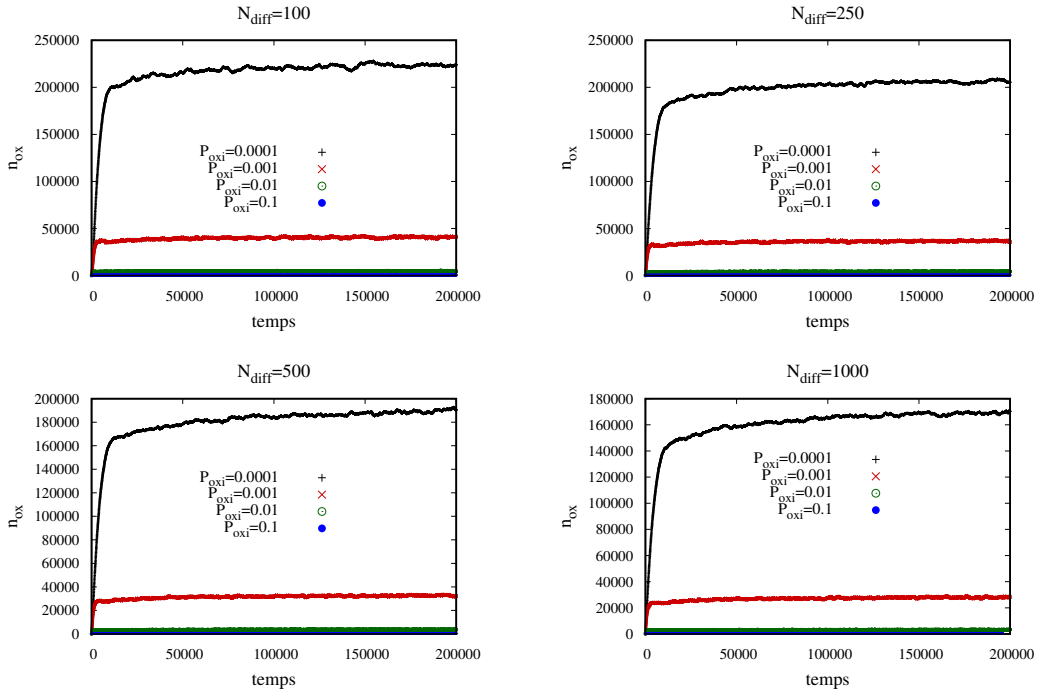

Figure 6: Evolution of oxide number for $N_{\rm diff} = 100, 250, 500$ and 1000 and different values of $P_{\rm oxi}$ indicated at each plot

sites for fixed values of $N_{\rm diff}$ and different values $P_{\rm oxi} = 0.0001$, 0.001, 0.01 and 0.1. As expected the dissolution probability $P_{\rm oxi}$ of the oxide has a direct strong effect on $n_{\rm ox}$. The higher the dissolution rate, the fewer the number of oxides on the surface. Figure 7 shows the evolution of the number of oxide sites for fixed values of $P_{\rm oxi}$ and different values of $N_{\rm diff} = 100$, 250, 500 and 1000. For instance for $P_{\rm oxi} = 0.0001$ and $N_{\rm diff} = 100$, there are $\approx 2.25\,10^5$ oxide sites formed on the metal which represents a coverage ratio of about 22% with respect the planar surface. For a variation of an order of magnitude of $N_{\rm diff} = 1000$, the number of oxides in stationary regime varies only of 25%, the effect is more limited. For all values of $P_{\rm oxi}$ presented, the variation is less than 50%. For $P_{\rm oxi} = 0.01$ and 0.1, when dissolution is quantitative, there are respectively only a few thousand and a few hundred sites of oxides negligible compared to the 10^6 sites on the

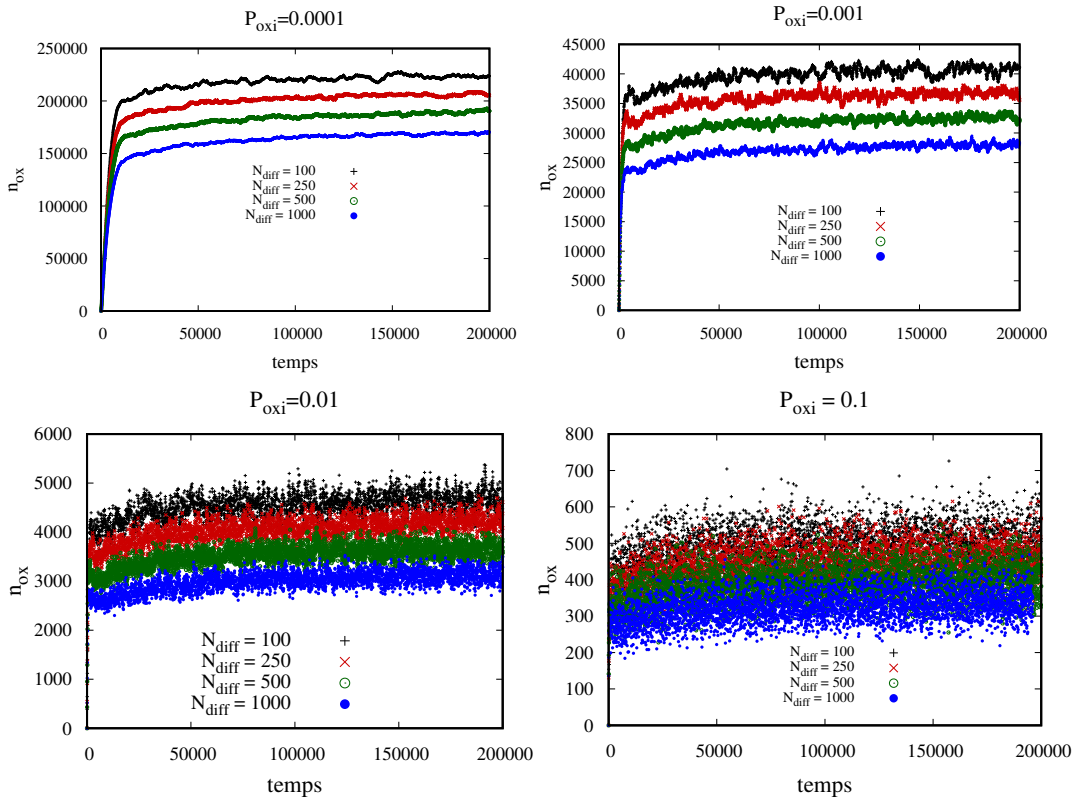

Figure 7: Number of oxide sites for $P_{\text{oxi}} = 0.0001, 0.001, 0.01$ and 0.1 and different values of N_{diff} indicated at each plot

surface. Typically 500 sites correspond to a coverage rate of 0.05 %, so the surface can hardly be considered passivated. The fluctuation of this number are in this case large.

Second, we present the stationary values of n_{ox} as a function of the parameters N_{diff} and P_{oxi}. Figure 8, we plot the stationary value of n_{ox} as a function of N_{diff} for different values P_{oxi}. A low dependence of the number of oxides with N_{diff} is noted in contrast to the effect of P_{oxi} which is clearly visible in figure 9. We consider on the plots that a coverage of less than 1 % corresponds to a no passivation regime. Figure 9 shows in a $\log - \log$ scale, the P_{oxi} dependence for different N_{diff} values. In this representation, we observe an almost a linear behavior with P_{oxi}. The linear fit of $\log(n_{\text{ox}})$ with the function $f(x) = a_1\, x + a_2$ is shown in Table 2. The standard error on the coefficients is around $3 - 4\,\%$ for a_1 and $5\,\%$ for a_2. As a first approximation, we observe that a_1 is close to -1, which corresponds to a behavior in inverse of the value of P_{oxi}. This behavior can be understood from a simple model. In the stationary state, we have a balance between production of oxide sites that we note δn_{ox} and their dissolution with a kinetic proportional to

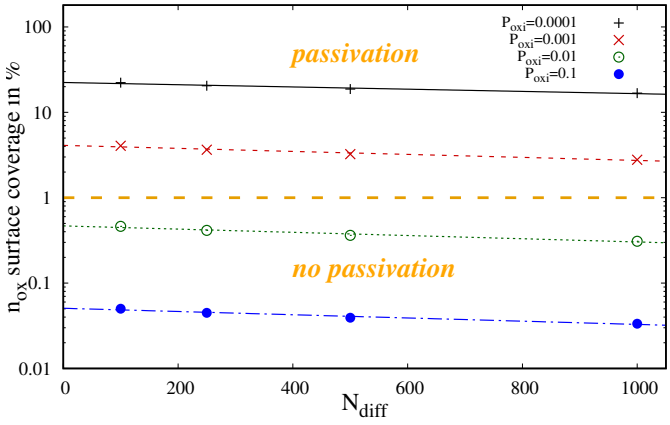

Figure 8: Coverage of the surface with oxide sites in % in stationary regime as a function of N_{diff} for different values of P_{oxi}. Orange dotted line separates passivated (above) and non passivated regimes (below).

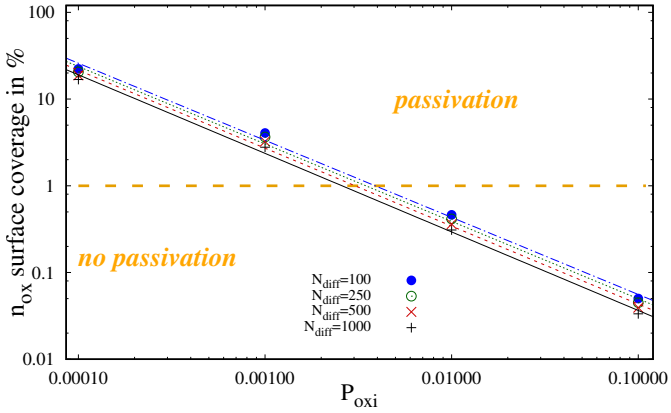

Figure 9: Coverage of the surface with oxide sites in % in stationary regime in a function of P_{oxi} for different values of N_{diff}. Orange dotted line separates passivated (above) and non passivated regimes (below).

their number n_{ox} and their probability of dissolution P_{oxi}. We recall that we study the effect of the dissolution parameter only in neutral medium due to slow corrosion. Always as a first approximation, we can assume that P_{oxi} parameter does not directly affect the corrosion thus δn_{ox} is independent of this parameter in this approximation. So, in the stationary state, we have an equilibrium between production δn_{ox} and dissolution $n_{\text{ox}} P_{\text{oxi}}$ of oxide sites which gives the relation

$$n_{\text{ox}} \approx \frac{\delta n_{\text{ox}}}{P_{\text{oxi}}} \tag{7}$$

This justifies the inverse depence of n_{ox} with P_{oxi}. In reality, for the different values of N_{diff}, on

Table 2: Fits for the function $f(x)$ function corresponding to figure 9.

N_{diff}	a_1	error	a_2	error
1000	-0.90575	3.4%	1.6566	5.2%
500	-0.89865	3.8%	1.7377	5.4%
250	-0.89260	4.1%	1.8046	5.5%
100	-0.88875	4.3%	1.8584	5.6%

average coefficient a_1 is closer to -0.89. This is so because the amount of oxide sites produced in the stationary state is not independent of P_{oxi}. Oxide sites are produced at metal reactive sites, the number of these sites depends on chemical roughness, on the dissolution rate of oxide sites therefore depends partly on the parameters P_{oxi} and N_{diff}. For small P_{oxi}, the number of oxide sites is larger on the surface, therefore the number of reactive sites is lower, which produce a smaller number of oxide sites δn_{ox}. In contrast, in the case of a fast dissolution, δn_{ox} increases as a function of P_{oxi}. Assuming that it can be written as a law of power, by putting such an expression in equation 7, we would obtain a lower exponent in absolute value of -1.

3.5. Oxygen concentration Effect

Previous studies on the corrosion of iron showed that corrosion is faster with increasing DO concentration [28]. However, the iron release in solution decreases with increasing the DO concentration [29]. The combined effects of corrosion, oxide production and dissolution and roughness may lead to complicated effects. In this part, we study the effect of the oxygen concentration on the kinetics of the corrosion process. An important point, in this paper, is to show that the limited flux of DO reaching the metal surface induces a slow corrosion rate due to a cathodic control of the corrosion. Corrosion rates for three oxygen concentrations will be presented. They do not correspond precisely to real systems because in normal pressure and temperature DO is already saturated for a few ppm. Such concentrations could be reached at higher pressures and temperatures like supercritical systems. The solubility of oxygen changes by 4 orders of magnitude in supercritical water at $500°C$ in [30, 31]. But we should also reconsider the values of other parameters such as diffusion coefficients. In [32], Xiao Ji et al., using molecular dynamic simulation, calculated the diffusion coefficient of oxygen, nitrogen and sodium chloride in supercritical water. They demonstrated that the diffusion coefficient of oxygen increases with the temperature. X. Zhao et al. used molecular dynamic simulation to calculate diffusion coefficient of O_2 [33] and water [34], at $300\,K$, $1\,atm$ and in supercritical conditions. Respectively

their diffusion coefficients at normal conditions are equal to $2.0\,10^{-5} cm^2/s$ and $2.1\,10^{-5} cm^2/s$. Whereas in supercritical conditions, they predict $811.2\,10^{-5} cm^2/s$ at $973\,K$ and $250\,atm$ for oxygen and $741.9\,10^{-5} m^2/s$ for water.

However a comparison with such systems is made difficult by the fact that besides DO concentration other parameters like diffusion coefficients also change. In the following, we consider three different DO concentrations assuming to simplify that all other parameters, like diffusion coefficients, remain identical. The aim is to focus on DO effects on corrosion only.

We present in figure 10, snapshots of the surface for $P_{\text{oxi}} = 0.0001$ and we choose the value of $N_{\text{diff}} = 250$. Snaphots for other values of N_{diff} are qualitatively similar. We see that with

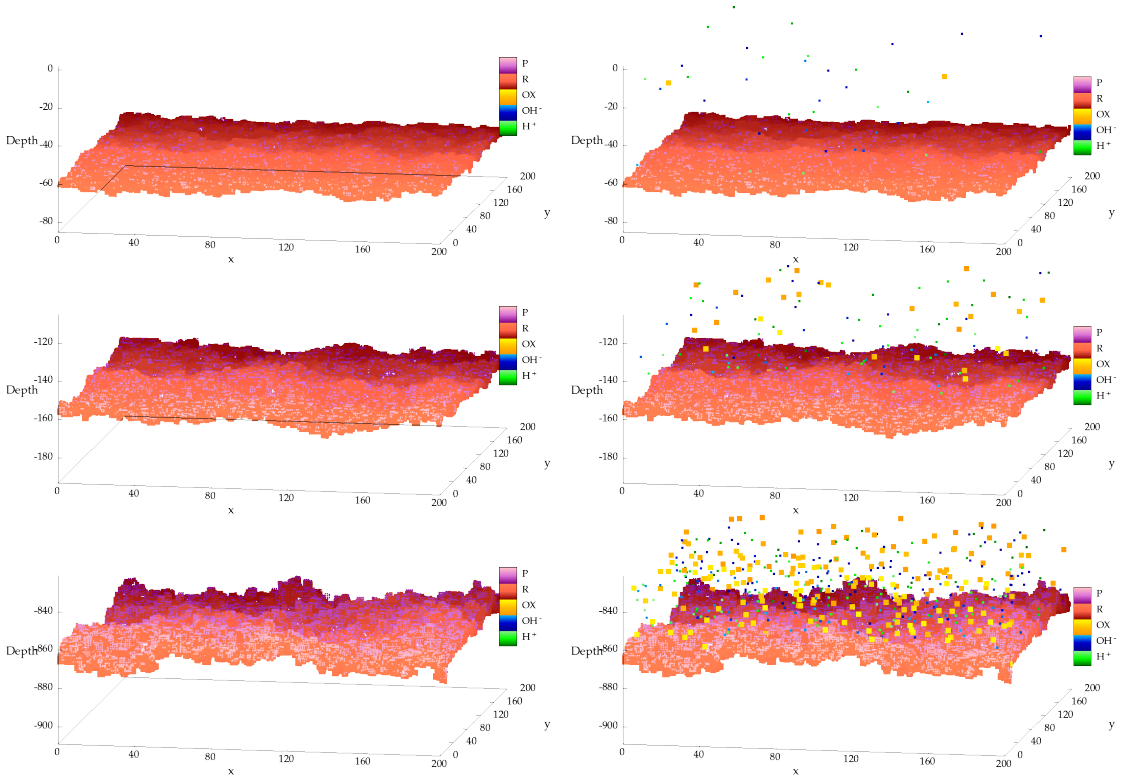

Figure 10: Corroded metallic surface, lines correspond to different DO concentration, from the top to the bottom: $c_{O_2} = 2.\,10^{-6}, 2.\,10^{-5}, 2.\,10^{-4}$ number of sites of the last plan that remain constant ($2.\,10^{-6}$ sites corresponds to $6ppm$ of DO (OX on the figure)). The left column only shows the metallic surface with R and P sites, the right column also DO, H^+ and OH^- sites.

the increase in the number of DO in solution, there is also an increase in the number of H^+ and OH^- sites and an increase in the surface roughness. This relates to the fact that when

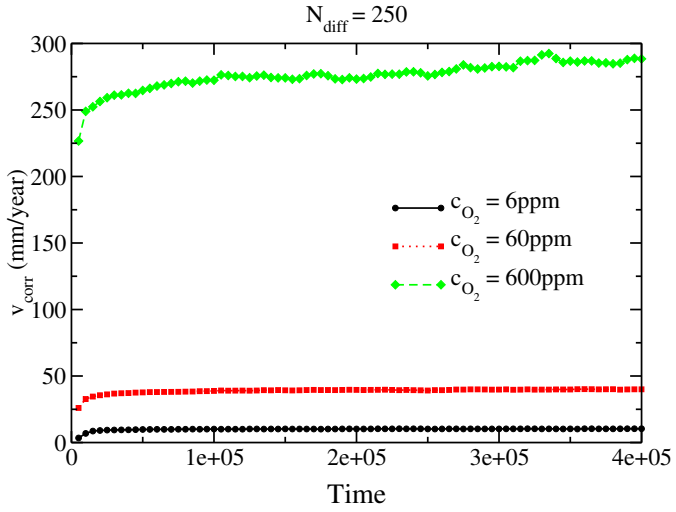

Figure 11: Corrosion rate for $N_{\text{diff}} = 250$, $P_{\text{oxi}} = 0.0001$ and different concentrations of oxygen.

we increase the oxygen concentration, we increase the number of electrochemical reactions with production of H^+ and OH^- ions. Also, with fixed P_{oxi} parameter, the number of oxide sites on the surface increases with DO in solution. Since the process is stochastic the formed oxide number are randomly distributed on the metallic surface, corrosion can occur only between the passivated sites contributing to an increase in surface roughness.

Figure 11 shows the evolution of the corrosion rate for given values $N_{\text{diff}} = 250$ and $P_{\text{oxi}} = 0.0001$ and different values of the oxygen concentration. We notice that the kinetic of the stationary state varies significantly with the oxygen concentration. For instance for c_{O_2} from 6ppm to 60ppm the corrosion rate is multiplied by 5. The precise dependence will be detailed below.

Figure 12 shows the corrosion rate of the stationary regime for $N_{\text{diff}} = 250$ and for the values $P_{\text{oxi}} = 0.0001, 0.001, 0.01$ and 0.1 as a function of the oxygen concentration in $\log - \log$ scale. We can see that we have approximately a scaling law with the concentration of oxygen, especially for large values of P_{oxi}. If we adjusts the $\log - \log$ scale with the linear function $f(x) = b_1\, x + b_2$ we obtain results in table 3 for the coefficients b_1 and b_2 for the different values of P_{oxi}. We can see that the regression is better for large values of P_{oxi} when the dissolution of the oxide leads to a few passivated regions of the metallic surface.

For small dissolution rate (small P_{oxi}), the oxide remains stable on the surface and thus protects the metal and slows its corrosion rate, which is visible of the corrosion rate figure 12. As

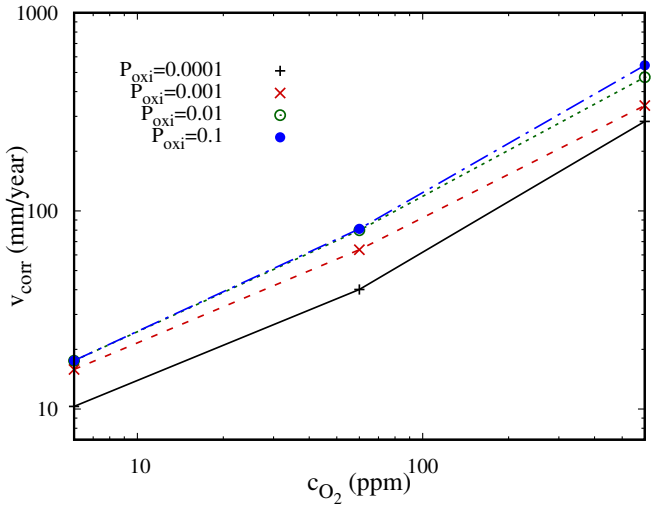

Figure 12: Corrosion rate in stationnary regime for different values of $P_{\text{oxi}} = 0.0001, 0.001, 0.01$ and 0.1 in a function of oxygen concentration Points corresponds to the adjustment of straight lines in $\log - \log$ scale.

Table 3: Parameters b_1 and b_2 for $f(x)$ to fit the corrosion rates of 12.

P_{oxi}	b_1	error	b_2	error
0.0001	0.71926	10%	5.069	7%
0.001	0.66584	5.4%	4,974	3.4%
0.01	0.71560	4.6%	5,303	3.0%
0.1	0.74529	6.2%	5.465	4.0%

mentionned earlier, the effect is negligible in the case of $P_{\text{oxi}} = 0.01$ and 0.1, for which there is a strong dissolution, the behavior is almost identical for small concentrations $c[O_2] = 2.10^{-6}$ and 2.10^{-5}. Since the amount of DO is low, few oxide sites are produced and for these two values of P_{oxi}, they are immediately dissolved. In the case of $c[O_2] = 2.10^{-4}$, there is a slight difference because the oxide production starts to be quantitative.

It can be seen that the corrosion rate depends on the concentration of oxygen. But the behavior is not linear with the oxygen concentration, it increases more slowly with a weaker exponent between 0.66 and 0.74. The corrosion rate with cathodic control from DO is modified due to the formation of the oxide. The corrosion rate is slowed down due to passivation. This effect increases with the concentration of DO. For a given P_{oxi}, the dissolution rate is fixed, but at the same time a larger DO concentration increases the production rate of oxides.

4. Comparison with experimental kinetics

In this Section, we compare the results of the model to experimentally measured weight loss of Fe_3O_4 in water in $50°C$ in experiences performed by D.C. Smith and B. McEnaney in [22]. For the weight loss and $4\,ppm$ of DO at $50°C$, they found a corrosion rate around $1.1mm/year$. In previous sections, we have shown how it is possible to model small oxygen concentrations like $6\,ppm$ and at the same time account for stoichiometric reactions. Here we aim for approximate comparison with experimental results. For computational reasons, to avoid fractional number of lattice sites in the last plane, we have made the calculations with a DO concentration of $6\,ppm$. In the future a fractional number of sites can be considered by introducing a probability of having 1 or 2 DO sites on the last plane. However, this solution has been ruled out here because of lengthy simulation times. With $6\,ppm$ of DO, diffusion step $N_{\text{diff}} = 1000$ and a dissolution probability in neutral solution $P_{\text{oxi}} = 0.001$ our simulations predicts a corrosion rate around $2.04\,mm/year$. For this value of $P_{\text{oxi}} = 0.001$, the coverage corresponds approximately to 2.6%, this value is consistent with the fact that iron does not strongly passivate. If we linearly rescale the $6\,ppm$ concentration results for $4\,ppm$ concentration, we would obtain a $1.36\,mm/year$ which is comparable to the $1.1mm/year$ value measured experimentally although higher. A lower value of current could mean a lower value of P_{oxi}. Another hypothesis is that we have neglected the Pilling Bedworth factor [35, 36] accounting for the fact that the oxide has a larger molar volume than the metal. The efficiency of the oxide to passivate the surface would then be greater. This effect is similar to a smaller value of P_{oxi} which also leads to a smaller current. For simplicity, this correction has not been accounted for in this work as simulation for one set of parameters are already long but will be considered in the future. Finally, note that in the absence of roughness the corrosion rate would be $0.75\,mm/year$ for a flat surface. This is smaller than the experimental value, which seems to confirm the role of roughness.

5. Conclusion

In this paper, we investigate a cellular automata model for aqueous corrosion accounting for spatially separate and balanced anodic and cathodic half reactions. In comparison to previous similar models, we account here for a cathodic reaction with dissolved oxygen. Cathodic control of corrosion is shown in relation with the flux of dissolved oxygen reaching the metallic surface. To our knowledge this is the first model providing an explicit mechanism accounting for this process. For low DO concentration, whether there is or not passivation, we remain in cathodic control regime determined by DO diffusion. On the contrary, for higher DO concentration there is a stronger effect of the passive layer on the kinetics.

To reach quantitative results, we have shown how to compel both stoechiometric corrosion reactions and small dissolved oxygen concentrations as those found in aqueous solutions within in the framework of a cellular automata approach. The scarcity of corrosion events requires long simulation times and intensive use of computational resources which have been implemented in parallel GPU simulations. Results of the model are comparable to experimental results and can be improved in the future by avoiding some approximations introduced for computational reasons.

The study shows the important role of the surface roughness, in relation to stochastic passivation on the metallic surface, on corrosion kinetics. This justifies the choice for stochastic cellular automata modelling in contrast to continous deterministic models like finite element approches [37, 38, 39, 40]. Different scaling laws have been obtained demonstrating the role of passivation on corrosion kinetics, both from a direct passivation effect of the surface or through a modification of the surface roughness.

Acknowledgment

M. Zenkri, F. Raouafi and D. di Caprio acknowledge the financial support by the *PHC Utique* program of the French Ministry of Foreign Affairs and Ministry of higher education and research and the Tunisian Ministry of higher education and scientific research in the CMCU project number 17G1207.

Data availability statement

The data that support the findings of this study are available from the corresponding author upon reasonable request

References

[1] G. Jacobson. International measures of prevention, application, and economics of corrosion technologies study. http://impact.nace.org/economic-impact.aspx, 2016.

[2] Iso 8044:2015, corrosion des mtaux et alliages. https://www.iso.org/obp/ui/#iso:std:iso:8044:ed-4:v1:en, 2015.

[3] F. Moulinier. Combien coûte la corrosion ? *TSM*, 7/8:26–38, 2010.

[4] ASM International. Handbook Committee. *ASM Handbook*. Number v. 13, pt. 2 in ASM Handbook. ASM International, 1990.

[5] A. Ismail and NH. Adan. Effect of oxygen concentration on corrosion rate of carbon steel in seawater. *American Journal of Engineering Research*, 3(1):64–67, 2014.

[6] N. Sato. Some concepts of corrosion fundamentals. *Corrosion science*, 27(5):421–433, 1987.

[7] R. Walter, M. Bobby Kannan, and M Bobby. Influence of surface roughness on the corrosion behaviour of magnesium alloy. *Materials & Design*, 32(4):2350–2354, 2011.

[8] T. Hong and M. Nagumo. Effect of surface roughness on early stages of pitting corrosion of type 301 stainless steel. *Corrosion science*, 39(9):1665–1672, 1997.

[9] Y. Zuo, H. Wang, and J. Xiong. The aspect ratio of surface grooves and metastable pitting of stainless steel. *Corrosion Science*, 44(1):25–35, 2002.

[10] W. Li and DY. Li. Influence of surface morphology on corrosion and electronic behavior. *Acta materialia*, 54(2):445–452, 2006.

[11] M. Cabrini, A. Cigada, G. Rondell, and B. Vicentini. Effect of different surface finishing and of hydroxyapatite coatings on passive and corrosion current of Ti6Al4V alloy in simulated physiological solution. *Biomaterials*, 18(11):783–787, 1997.

[12] R. B. Alvarez, Holly J. Martin, MF. Horstemeyer, Mei.Q. Chandler, N. Williams, Paul T. Wang, and A. Ruiz. Corrosion relationships as a function of time and surface roughness on a structural AE44 magnesium alloy. *Corrosion Science*, 52(5):1635–1648, 2010.

[13] L. Abosrra, Ashraf Ashour, S. Mitchell, and Mansour Youseffi. Corrosion of mild steel and 316L austenitic stainless steel with different surface roughness in sodium chloride saline solutions. In *EUROCORR 2009*, volume 65, pages 161–172, 06 2009.

[14] P. Meakin, T. Jøssang, and J. Feder. Simple passivation and depassivation model for pitting corrosion. *Physical Review E*, 48(4):2906, 1993.

[15] C. F. Pérez-Brokate, D. Di Caprio, D. Féron, J. de Lamare, and A. Chaussé. Overview of Cellular Automaton Models for Corrosion. In *Cellular Automata*, number 8751 in Lecture Notes in Computer Science, pages 187–196. Springer International Publishing, January 2014.

[16] M. Zenkri, D. Di Caprio, C. F. Pérez-Brokate, D. Féron, J. de Lamare, A. Chaussé, , F. Larbi, and F. Raouafi. Contribution of cellular automata to the understanding of corrosion phenomena. *Condens. Matt. Phys.*, 20:33802:1–13, 2017.

[17] C.F. Pérez-Brokate, D. di Caprio, D. Féron, J. de Lamare, and A. Chaussé. Three dimensional discrete stochastic model of occluded corrosion cell. *Corrosion Science*, 111:230 – 241, 2016.

[18] C.F. Pérez-Brokate, D. di Caprio, D. Féron, J. de Lamare, and A. Chaussé. Probabilistic cellular automata model of generalized corrosion, transition to localized corrosion. *Corrosion Engineering, Science and Technology*, 52–51:186–193, 2017.

[19] C.F. Pérez-Brokate, D. di Caprio, D. Féron, J. de Lamare, and A. Chaussé. Pitting corrosion modelling by means of a stochastic cellular automata-based model. *Corrosion Engineering, Science and Technology*, 52(8):605–610, 2017.

[20] D. Stauffer and A. Aharony. *Introduction to percolation theory*. Taylor & Francis, London, 2nd edition, 1994.

[21] E. Schaschl and G.A. Marsh. The effect of dissolved oxygen oon corrosion steel and on current required for cathodic protection. *Corrosion*, 13(4):35–43, 1957.

[22] D.C. Smith and B. McEnaney. The influence of dissolved oxygen concentration in the corrosion of grey cast iron in water at 50° C. *Corrosion Science*, 19:379–394, 1979.

[23] C.F. Pérez-Brokate, D. di Caprio, E. Mahé, D. Féron, and J. de Lamare. Cyclic voltammetry simulations with cellular automata. *Journal of Computational Science*, 11:269–278, November 2015.

[24] R. T. Ferrell and D. M. Himmelblau. Diffusion coefficients of nitrogen and oxygen in water. *Journal of Chemical & Engineering Data*, 12(1):111–115, 1967.

[25] G. Engelhardt, M. Urquidi-Macdonald, and D. D. Macdonald. A simplified method for estimating corrosion cavity growth rates. *Corrosion Science*, 39(3):419–441, March 1997.

[26] D. di Caprio and J. Stafiej. Effect of low oxygen concentration on the oxidation behavior of Ni-based alloys 625 and 825 in supercritical water. *Electrochimica Acta*, 54:3884–3890, 2010.

[27] D. di Caprio and J. Stafiej. Effect of low oxygen concentration on the oxidation behavior of Ni-based alloys 625 and 825 in supercritical water. *Electrochimica Acta*, 56:3963–3968, 2011.

[28] G. Gedge. Corrosion of cast iron in potable water service. In *Proc. corrosion and related aspects of materials for potable water supplies, proceedings of the institute of materials conference.* London, UK, 1992.

[29] Laurie S McNeill and Marc Edwards. Iron pipe corrosion in distribution systems. *Journal-American Water Works Association*, 93(7):88–100, 2001.

[30] X. Tang, S. Wang, L. Qian, Y. Li, Z. Lin, D. Xu, and Y Zhang. Corrosion behavior of nickel base alloys, stainless steel and titanium alloy in supercritical water containing chloride, phosphate and oxygen. *Chemical Engineering Research and Design*, 100:530–541, 2015.

[31] J. Yang, S. Wang, X. Tang, Y. Wang, and Y. Li. Effect of low oxygen concentration on the oxidation behavior of Ni-based alloys 625 and 825 in supercritical water. *The Journal of Supercritical Fluids*, 131:1–10, 2018.

[32] Xiao Ji, Lu Jiu-Fang, Chen Jian, and Li Yi-Gui. Molecular dynamics simulation of diffusion coefficients of oxygen, nitrogen and sodium chloride in supercritical water. *Chinese Physics Letters*, 18(7):847, 2001.

[33] Xiao Zhao, Yuanxue Liu, Jian Zou, Qiuxia Wang, Hao Liu, Hua Zhang, and Hui Jin. Determining diffusion coefficients of oxygen in supercritical water with molecular dynamics. *Thermal Science*, 23:781–787, 2019.

[34] Xiao Zhao and Hui Jin. Investigation of hydrogen diffusion in supercritical water: A molecular dynamics simulation study. *International Journal of Heat and Mass Transfer*, 133:718–728, 2019.

[35] D. Di Caprio, C. Vautrin-Ul, J. Stafiej, J. Saunier, A. Chaussé, D. Féron, and J.P. Badiali. Morphology of corroded surfaces: Contribution of cellular automaton modelling. *Corrosion Science*, 53(1):418–425, 2011.

[36] C. Xu and W. Gao. Pilling-bedworth ratio for oxidation of alloys. *Material Research Innovations*, 3(4):231–235, 2000.

[37] D. R. Gunasegaram, M. S. Venkatraman, and I. S. Cole. Towards multiscale modelling of localised corrosion. *International Materials Reviews*, 59(2):84–114, 2014.

[38] Digby D. Macdonald. The history of the Point Defect Model for the passive state: A brief review of film growth aspects. *Electrochimica Acta*, 56(4):1761–1772, January 2011.

[39] F. Thébault, B. Vuillemin, R. Oltra, C. Allely, and K. Ogle. Modeling bimetallic corrosion under thin electrolyte films. *Corrosion Science*, 53(1):201 – 207, 2011.

[40] F. Thébault, B. Vuillemin, R. Oltra, C. Allely, and K. Ogle. Reliability of numerical models for simulating galvanic corrosion processes. *Electrochimica Acta*, 82(Supplement C):349 – 355, 2012. Electrochemical frontiers in global environment and energy.